Input-Reflectionless Acoustic-Wave-Lumped-Element Resonator-Based Bandpass Filters

Dimitra Psychogiou[1], Dakotah J. Simpson[1], and Roberto Gómez-García[2]
[1]University of Colorado at Boulder, Boulder, CO 80309, USA
[2]University of Alcalá, Alcalá de Henares 28871, Spain

***Abstract*—This paper reports on an RF design methodology for acoustic-wave-resonator-(AWR)-based bandpass filters (BPFs) with input-reflectionless behavior in both their passband and stopband regions. The proposed concept is based on acoustic-wave-lumped-element resonators (AWLRs) that are incorporated in series-cascaded reflectionless stages (RLSs). Each RLS comprises a first-order bandpass section—shaped by three impedance inverters and one AWLR—and a first-order resistively-terminated bandstop section—shaped by two impedance inverters and one AWLR—that are designed to exhibit complementary transfer functions. In this manner, an input-reflectionless behavior can be obtained both at the passband and stopband regions of the filter. In addition, the use of AWLRs in the RLSs facilitates the realization of high-quality-factor (Q> 10,000) quasi-elliptic-type transfer functions with fractional bandwidths (FBWs) that are wider than the electromechanical coupling coefficient (k_t^2) of its constituent AWRs. For proof-of-concept validation purposes, one- and two-state prototypes were manufactured, and measured at 418 MHz using commercially-available surface-acoustic-wave resonators.**

***Index Terms*— Acoustic-wave (AW) filter, bandpass filter (BPF), high-quality-factor (Q) filter, k_t^2 enhancement, reflectionless filter, RF/microwave filter, surface-acoustic-wave resonator.**

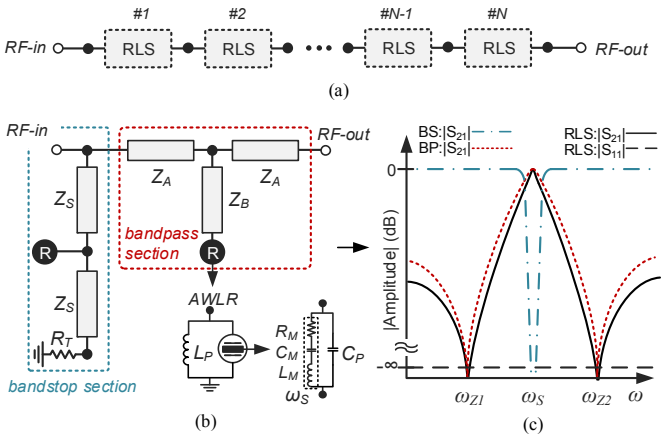

Fig. 1. Input-reflectionless AWLR-based BPF concept. (a) Block diagram of an N-stage input-reflectionless AWLR-based BPF that is shaped by N series-cascaded RLSs. (b) Circuit schematic of the RLS and detail of the AWLR (R) that is shaped by one AWR and a lumped-element inductor L_P. (c) Conceptual power transmission and reflection responses of the proposed RLS and its corresponding BS and BP sections.

I. Introduction

Emerging wireless-communication systems, including 5G, are increasingly calling for sophisticated RF hardware that can enhance the signal-to-noise ratio (SNR) of their RF front-ends and facilitate the reception of weak signals in the presence of undesired interference [1]. Among the fundamental devices, highly-selective bandpass filters (BPFs) with as minimum as possible input reflection both at their passband and stopband regions—i.e., input-reflectionless or absorptive BPFs—are of critical importance for the realization of high SNR.

Despite the significance of this type of filters, there has been a limited number of input-reflectionless BPFs in the open technical literature. These include: i) lumped-element BPFs that are based on symmetrical configurations with complementary even/odd-mode input-reflection properties [2] and ii) microstrip/lumped-element architectures that are formed by resistively-terminated duplexers [3], [4]. However, none of these concepts meets the high levels of compactness and stringent insertion-loss (IL) requirements of wireless-communication transceivers due to their low quality factor (Q)—20-150 in [2]-[4]—and/or large physical size of their constituent resonators.

Acoustic-wave-resonator-(AWR)-based RF filters, such as those using surface-acoustic-wave (SAW) and bulk-acoustic-wave (BAW) resonators, have been the key RF filtering elements in wireless-communication RF front-ends due to their high Q (>1,000) and small volume (1-4 mm^3/resonator) [5]. However, none of the conventional ladder, lattice, or self-cascaded configurations facilitate the realization of reflectionless stopband regions. In addition, their fractional bandwidth (FBW) is limited by the electromechanical coupling coefficient (k_t^2) of the AWRs and is typically around $0.6k_t^2$ [5]-[7].

In this paper, a new class of AWR-based BPFs is proposed with the following characteristics: i) input-reflectionless behavior both at their passband and stopband regions and ii) quasi-elliptic-type transfer functions with enhanced FBW, i.e., >$0.6k_t^2$. The proposed filter concept is based on acoustic-wave-lumped-element resonators (AWLRs) [8] and series-cascaded reflectionless stages (RLS) that are shaped by bandpass and bandstop sections with complementary transfer functions.

The content of this paper is organized as follows. Section II presents the RF design principles of the input-reflectionless AWLR-based BPF concept. Proof-of-concept demonstrators consisting of one- and two-stage prototypes are shown in Section III. Finally, a summary of the relevant contributions of this work is given in Section IV.

II. Filter Concept and Theoretical Foundations

The details of the AWLR-based input-reflectionless BPF concept are shown in Fig. 1. It is based on N series-cascaded RLSs and exhibits input-reflectionless behavior both at its passband and stopband regions as well as a quasi-elliptic-type power-transmission response. Each RLS consists of a first-order bandpass (BP) section—shaped by three impedance inverters and one AWLR—and a resistively-terminated first-order bandstop (BS) section—shaped by two impedance inverters and one AWLR—that have complementary transfer functions as shown in Fig. 1(b) and (c). In this manner, the BP section determines the overall power-transmission response of the RLS and the reflected power at its stopband regions is dissipated in the resistive termination of the BS section. In order to achieve input-reflectionless behavior both at the passband and stopband regions of the RLS—i.e., S_{11}=0 for $\forall f$—its impedance inverter's values need to satisfy (1) where Z_O denotes the system's reference impedance.

$$Z_S=Z_B Z_O/Z_A \tag{1}$$

The obtained quasi-elliptic-type power-transmission response of the RLS is due to the use of AWLRs that exhibit one pole at ω_S and two transmission zeros (TZs) at ω_{Z1} and ω_{Z2}, Fig. 1(c). In particular, the pole appears at the series resonant frequency of the AWR, whose equivalent Butterworth-Van-Dyke (BVD) model is shown in Fig. 1(b). The two TZs appear at frequencies in which the input impedance of the AWLR—shaped by one AWR and a lumped-element inductor L_P that resonates with the AWR's parallel capacitance C_P at ω_S—is infinite as discussed in [8]. As such, the overall power-transmission response of an N-stage AWLR-based input reflectionless BPF exhibits N poles and $2N$ TZs.

The basic design aspects of the input-reflectionless AWLR-based BPF concept are shown in Fig. 2 through various examples of theoretically-synthesized responses. In particular, Fig. 2(a) illustrates the theoretical power transmission and reflection responses of a RLS that comprises AWRs with k_t^2=0.077%—a typical value for commercially-available SAW resonators—for various levels of Z_B/Z_A. It can be seen that the increase of Z_B/Z_A results in wider FBWs that can be designed to be larger than k_t^2 unlike conventional ladder, lattice, or self-cascaded AWR-based BPFs architectures with FBWs around $0.6k_t^2$. A comparison between the RLS's responses using ideal inverters and inverters shaped by 90°-long transmission lines (TLs) is also shown in the same figure. It can be seen that in the realistic implementation—TL inverters—, the magnitude of the input reflection of the RLS is theoretically zero at the design frequency and exhibits a quasi-reflectionless behavior (red dashed line) elsewhere. Note that the input-reflection characteristics of the design cases in which ideal inverters are used are not shown in this figure due to being theoretically zero (infinite in dB scale) throughout the entire frequency range. Furthermore, it can be observed that the TL inverters move the TZs of the power transmission response closer to the BPF's center frequency. In Fig. 2(b), the theoretical response of various AWLR-based BPFs shaped by a different number of RLS are plotted. It is observed that the selectivity of the power transmission response can be increased by readily cascading in series multiple RLSs.

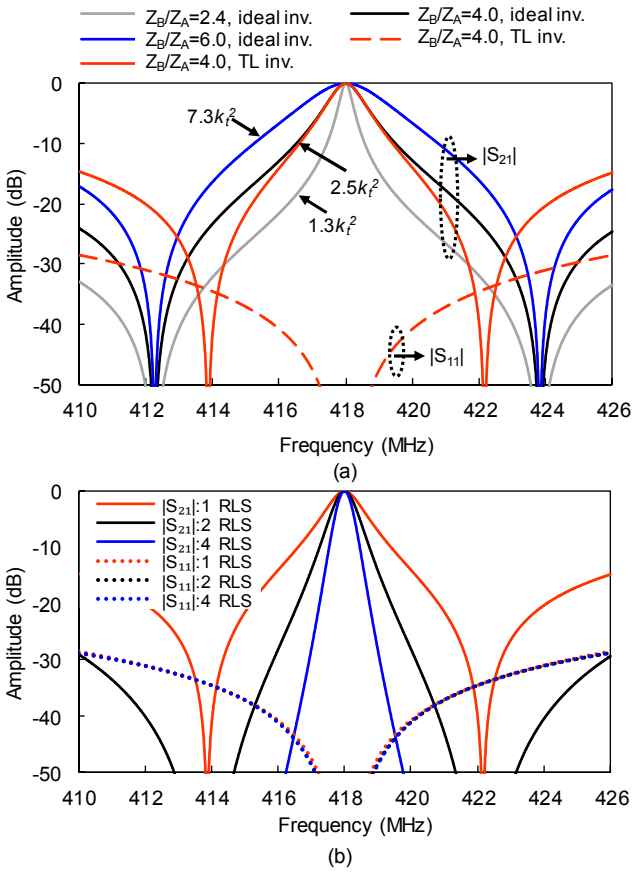

Fig. 2. (a) Theoretical power transmission and reflection responses of a one-stage input-reflectionless AWLR-based BPF that comprises AWRs with k_t^2=0.077% for various levels of Z_B/Z_A and ideal and TL-based impedance inverters. (b) Theoretical power transmission response for alternative number of RLSs and Z_B/Z_A=4. The RLSs are shaped by TL inverters.

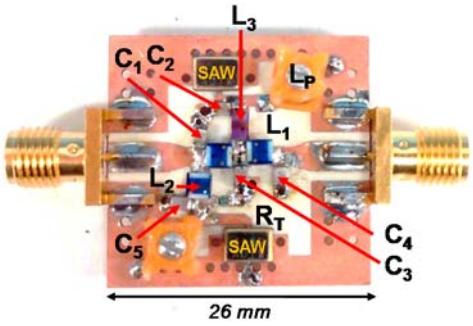

Fig. 3. Manufactured prototype of the one-stage input-reflectionless AWLR-based BPF. All impedance inverters were implemented with their first-order π-type circuit equivalent that comprises one series inductor from Coilcraft Inc. and two capacitors from Johanson Tech. The employed commercial components are as follows: L_1= 1008HQ33N, L_2= 1008HQ39N, L_3= 1206CS680, L_P=164-03A06L, C_1= 251R15S7R5CV4S, C_2= 251R15S1R8BV4S, C_3=251R15S9R1CV4S, C_4= 251R15S3R3BV4S, C_5= 251R15S3R6BV4S, R_T=TNPW0603237RBEEA00.

III. Experimental Validation

The RF design principles of the devised input-reflectionless AWLR-based BPF concept were experimentally validated through the design and manufacturing of two prototypes corresponding to one- and two-stage input-reflectionless AWLR-based BPFs. Both filters were built on a Rogers 4350B dielectric substrate with: dielectric permittivity ε_r=3.48, dielectric thickness H=1.52 mm, loss tangent tan(δ_D)=0.0024, and 35-µm-thick Cu-cladding. The filter design was performed with post-layout electromagnetic (EM) simulations using the Advanced Design System (ADS) software package while taking into consideration the design principles detailed in Section II. For practical-implementation purposes, each impedance inverter has been realized with its first-order π-type circuit equivalent. For size compactness, the loading resistor in the BS section was directly connected to the AWLR after being transformed by its preceding impedance inverter. Furthermore, commercially-available SAW resonators were used as AWRs. Both filters were designed for a center frequency of 418 MHz and FBW around $1k_t^2$.

The manufactured prototype of the one-stage input-reflectionless AWLR-based BPF and its constitutent commercially-available surface-mount elements are shown in Fig. 3. Its RF performance was experimentally validated with a Keysight N5224A PNA and is summarized in Fig 4. It exhibits the following RF performance metrics: 3-dB-bandwidth (BW) of 0.32 MHz, FBW of $1k_t^2$, minimum in-band IL of 0.98 dB that corresponds to an effective quality factor (Q_{eff}) >10,000, and return loss (RL) >26 dB throughout its entire passband and stopband regions. A comparison with the EM simulated response is also shown in the same figure for AWRs represented by their single-mode BVD model and the multi-mode model in [8] that predicts the presence of spurious modes at the theoretical level. As it can be seen, they are in a fair agreement and successfully validate the operating principles of the proposed filter concept. The manufactured prototype and RF-measured/simulated response of the two-stage prototype are respectively shown in Figs. 5 and 6. It exhibits a 3-dB BW of 0.32 MHz, FBW of $1k_t^2$, minimum in-band IL of 2.16 dB that corresponds to an effective quality factor (Q_{eff}) >10,000, and

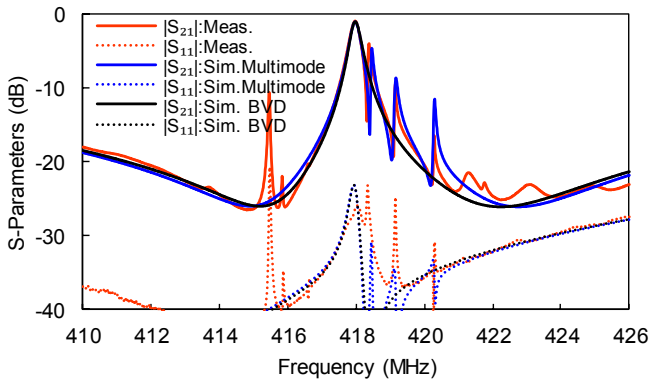

Fig. 4. RF-measured and EM-simulated S-parameters of the one-stage input-reflectionless AWLR-based BPF.

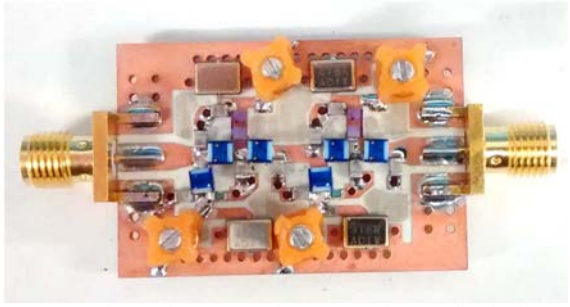

Fig. 5. Manufactured prototype of a two-stage input-reflectionless AWLR BPF—i.e., two in-series-cascaded RLSs—. It features the same component values as the ones listed in the one-stage prototype in Fig. 3.

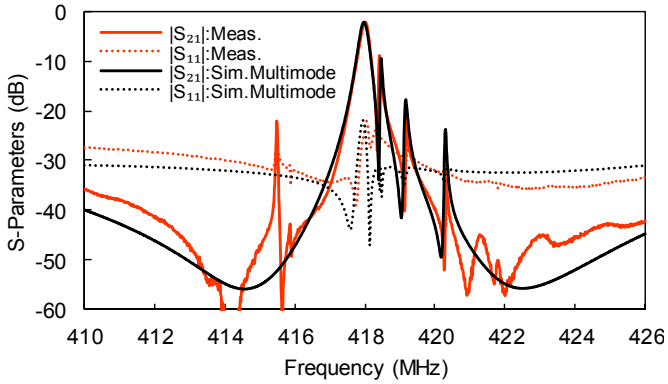

Fig. 6. RF-measured and EM-simulated S-parameters of the two-stage input-reflectionless AWLR-based BPF—i.e., two in-series-cascaded RLSs—.

RL >22 dB throughout its entire passband and stopband range. As expected, its selectivity is higher than in the one-stage circuit which validates the scalability of this filter concept to in-series-cascade multi-stage realizations.

IV. Conclusion

This paper has discussed the RF design principles of a new family of input-reflectionless AWLR-based BPFs. They are based on in-series-cascaded RLSs that comprise complementary BP and BS sections that are shaped by AWLRs and impedance inverters. The proposed configuration demonstrates for the first time the ability to realize enhanced-FBW—i.e., FBW> $0.6k_t^2$—AWR-based BPFs with input-reflectionless behavior both at their stopband and passband regions. The operational principles of the devised input-reflectionless AWLR-based BPF concept were experimentally validated at 418 MHz through the testing of two filter prototypes with the following characteristics: one-stage prototype with 3-dB BW of 0.32 MHz (FBW: $1k_t^2$), IL of 0.98 dB (Q_{eff} >10,000), and RL> 26 dB, and two-stage prototype with 3-dB BW of 0.32 MHz ($1k_t^2$), minimum IL of 2.16 dB (Q_{eff}>10,000), and RL >22 dB.

Acknowledgment

This work has been supported in part by the National Science Foundation under Grant no. 1731956 and the Dean's Graduate

Assistantship (DGA) of the University of Colorado at Boulder. The authors would like to thank Keysight for providing access to the software package Advanced Design System.

REFERENCES

[1] M. Rais-Zadeh, J. T. Fox, D. D. Wentzloff, and Y. B. Gianchandani, "Reconfigurable radios: A possible solution to reduce entry costs in wireless phones," *Proc. IEEE*, vol. 103, no. 3, pp. 438–451, Mar. 2015.

[2] M. A. Morgan and T. A. Boyd, "Reflectionless filter structures," *IEEE Trans. Microw. Theory Techn.*, vol. 63, no. 4, pp. 1263–1271, Apr. 2015.

[3] T.-H. Lee, B. Lee, and J. Lee, "First-order reflectionless lumped-element lowpass filter (LPF) and bandpass filter (BPF) design," in *IEEE MTTS Int. Microw. Symp. Dig.,* San Francisco, CA, USA, May 2016, pp. 1–4.

[4] D. Psychogiou and R. Gómez-García, "Reflectionless adaptive RF filters: bandpass, bandstop, and cascade designs," *IEEE Trans. Microw. Theory Techn*., vol. 65, no. 11, pp. 4593-4605, Aug. 2017.

[5] C. W. Ruppel, "Acoustic wave filter technology-A review" *IEEE Trans. Ultrasonics, Ferroelectrics, and Frequency Control (TUFFC)*, vol. 64, no. 9, pp. 1390-1400, Apr. 2017.

[6] S. Lee and A. Mortazawi, "An intrinsically switchable ladder-type BST-on-Si composite FBAR filter," *IEEE Trans. Ultrasonics, Ferroelectrics, and Frequency Control (TUFFC)*, vol. 63, no. 3, pp. 456-462, Jan. 2016.

[7] S. Gong and G. Piazza, "Design and analysis of Lithium-Niobate-based high electromechanical coupling RF-MEMS resonators for wideband filtering," *IEEE Trans. Microw. Theory Techn.*, vol. 61, no. 1, pp. 403–414, Jan. 2013.

[8] D. Psychogiou, R. Gómez-García, and D. Peroulis, "Coupling-matrix based design of high-*Q* bandpass filters using acoustic-wave lumped-element resonator (AWLR) modules," *IEEE Trans. Microw. Theory Techn.*, vol. 63, no. 12, pp. 4319–4328, Dec. 2015.